RSC Advances

PAPER

View Article Online
View Journal | View Issue



Cite this: *RSC Adv.*, 2017, **7**, 2905

# Self-assembled PEG–carboxymethylcellulose nanoparticles/α-cyclodextrin hydrogels for injectable and thermosensitive drug delivery†

Lin Dai,*[a] Rui Liu,[a] Li-Qiu Hu,[a] Jun-Hui Wang[b] and Chuan-Ling Si[abcd]

Received 25th October 2016
Accepted 28th November 2016

DOI: 10.1039/c6ra25793c

www.rsc.org/advances

Novel cellulose hydrogels based on the inclusion complex between α-cyclodextrin and binary-drug loaded nanoparticles (carboxymethylcellulose–betulinic acid/hydroxycamptothecine nanoparticles) were prepared in aqueous media for the first time. As the reversible supramolecular assembly behavior, the thermosensitive hydrogels showed distinctive reversible gel–sol transition properties related to structure at a particular temperature. The temperature of the gel–sol transition was decided by the concentration between the nanoparticles and α-cyclodextrin. In addition, the injectable drug delivery applications of the BA/HCPT-loaded hydrogel showed more effectively than that of free drugs and BA/HCPT-loaded nanoparticles for *in vitro* and *in vivo* studies. Such an injectable hydrogel with a unique structure and temperature responses would be a promising candidate for many intelligent delivery applications.

## 1. Introduction

Hydrogels are fascinating and versatile soft materials with three-dimensional cross-linked networks.[1] Because of the attractive properties and strong application potential, hydrogels are widely employed in drug delivery, cell immobilization and histological engineering. As one of the branch in gel chemistry, supramolecular polymer hydrogels have aroused particularly intensive concern in consideration of stimuli-responsiveness to noncovalent units.[2–4] Despite the huge potential of stimuli-responsive hydrogels, in many cases these systems have limited use as drug delivery platforms today, since they exhibit a relatively rapid release of hydrophilic drugs from the gel and inefficient hydrophobic drug loading.[5]

Polymeric nanoparticles have been a new kind of intelligent drug carrier for insoluble or amphiphilic drugs since 1984,[6–8] which shows a lot of obvious advantages such as structural and functional diversity, high drug loading capacity, long plasma half-life, and tunable degradation time for controlled drug delivery.[9,10] Indeed, polymeric nano-deliveries have many merit, but there are problems not we overlook such as the safety and stability.[11] Recently, based on the properties of polymeric nanoparticles and supramolecular polymer hydrogels, nanocomposite hydrogels is designed and prepared by combing the nano-materials and hydrogels to improve the performance biomedicine fields.[12,13] Supramolecular polypseudorotaxane (PPR), which is a classical model of supramolecular self-assembly, formed between cyclodextrins (CDs) and polymeric nanoparticles was thought to generate structural diversity as well as a major of property enhancements.[14] Strong hydrogen bonds between the adjacent threaded CDs result in microcrystalline aggregation and then promote physical gel formation.[15,16] It has been reported that the threading–dethreading process of PPR is a thermosensitive dynamic equilibrium, and the threading–dethreading transition temperature can be affected by the length of PEG chain and concentration of α-CD,[17,18] which endows the PPR hydrogel with tunable temperature-responsive potentials. Furthermore, these nanocomposite hydrogels showed significant efficacy in inhibition of tumor growth *in vivo*.

We have previously developed carboxymethylcellulose–betulinic acid (CMC–BA) prodrugs.[19] In this work, the amphiphilic prodrug CMC–BA and hydroxycamptothecine (HCPT) self-assembled into nanoparticles, and then with α-CD to form supramolecular hydrogels for injectable and thermosensitive drug delivery. Nanoparticles can promote the insoluble drug loading capacity of hydrogels, which can be modulated in a versatile way, with the modification of the nanoparticles. Moreover, the hybrid systems could enable routes of drug administration with limited systemic absorption but that can be useful in long term delivery systems. On the other hand, the injectable and thermosensitive hydrogels could be achieved by varying the concentrations of prodrugs and α-CD, and also

[a]*Tianjin Key Laboratory of Pulp and Paper, Tianjin University of Science and Technology, Tianjin 300457, China. E-mail: dailin@tust.edu.cn; Fax: +86-22-60602226; Tel: +86-22-60602226*

[b]*State Key Laboratory of Tree Genetics and Breeding, Research Institute of Forestry, Chinese Academy of Forestry, Beijing 100091, China*

[c]*Jiangsu Province Biomass Energy and Materials Laboratory, Institute of Chemical Industry of Forest Products, CAF, Nanjing 210042, China*

[d]*State Key Laboratory of Pulp and Paper Engineering, South China University of Technology, Guangzhou 510640, China*

† Electronic supplementary information (ESI) available. See DOI: 10.1039/c6ra25793c

provide nanoparticles with the clinically useful formulation needed for their clinical applications.

## 2. Experimental details

### 2.1. Reagents and materials

Sodium carboxymethylcellulose (CMC-Na) (degree of substitution = 0.82, $M_W$ = 275 kDa, FDA and EU food grade) was obtained from Sigma-Aldrich. Methoxy poly(ethylene glycol) carboxyl (M-PEG-COOH, $M_W$ = 2 kDa) was purchased from JenKem Technology Co., Ltd. (Beijing, China). Betulinic acid (BA) and hydroxycamptothecine (HCPT) were obtained from Preferred Biotechnology Co., Ltd (Sichuan, China). *N*-Hydroxysuccinimide (NHS), 4-dimethylaminopyridine (DMAP), and 1-ethyl-3-(3-dimethylaminopropyl)-carbodiimide HCl (EDC HCl) were purchased from Sigma Aldrich. Ultracentrifugation filters (Vivaspin MWCO 2 kDa, 3.5 kDa and 10 kDa) were bought from Fisher (Ottawa, ON, Canada).

Fetal bovine serum (FBS), Dulbecco's Modified Eagle's Medium (DMEM), penicillin, streptomycin, and Dulbecco's Phosphate-Buffered Saline (DPBS) were all purchased from Gibco. Cell-Counting Kit-8 (CCK-8) kit was received from the Dojindo Laboratories. The LLC cells were cultured by DMEM with 10% FBS, 1% streptomycin–penicillin and incubated in 5% $CO_2$/95% air humidified atmosphere at 37 °C.

### 2.2. Animals and ethics

C57BL/6 mice (female) ranging in age from 6 to 7 weeks obtained from Beijing HFK Bioscience Co., Ltd. were maintained in the animal house of Institute of Process Engineering (Chinese Academy of Sciences, Beijing, China) in a controlled environment (22 ± 2 °C, 55 ± 5% relative humidity, a 12 h light/dark cycle). All of the animal experiments were in accordance with the guidelines set by the National Institutes of Health (NIH Publication No. 85-23, revised 1985) and were approved by the Experimental Animal Ethics Committee, Beijing.

### 2.3. Characterization

The chemical construction of prodrugs was dissolved in deuterated chloroform ($CDCl_3$) and measured by $^1$H-NMR (DRX-600 Avance III spectrometer, Bruker). The rheological behaviours of the samples were analyzed by a rotational rheometer (Malvern Kinexus pro+). For the TEM (JEM-100CXa) analysis nanoparticles were diluted 50 to 100 times in deionized water, and then dropped onto the surface of a TEM copper grid with formvar film and naturally air dried before analysis at an acceleration voltage of 100 kV. The hydrogel samples were vacuum freeze dried and ground into a fine powder, and then placed on the conductive tape, coated with gold vapor for the SEM (Hitachi S-3400N II electron microscope) observations.

### 2.4. Formation of hydrogels

The CMC–BA prodrug was synthesized according to previously described methods.[19] CMC–BA prodrug containing 29.46 ± 2.35 wt% BA was obtained. The hydrogels were prepared between α-CD and the PEG chains of CMC–BA *via* the host–guest inclusion complexation in two steps. The brief preparation process for the hydrogel is as follows: 0.2 g CMC–BA prodrug and 0.1 g HCPT thoroughly dissolve in 0.2 mL of DMSO and then cautiously added, dropwise, into a rapidly vortexing PBS solution (3.8 mL, pH 7.4). The CMC–BA/HCPT NPs solutions were obtained after continue beating for 1 min, then transferred to a MWCO 10 kDa cartridge, and dialyzed for 12 h with two exchanges of dialysate against PBS solution (pH 7.4, 100 mL), and freeze-dried to obtained the particles. Secondly, different concentration of α-CD (1 mL, 100 to 150 mg mL$^{-1}$) was added into CMC–BA/HCPT NPs solutions (1 mL, 100 to 300 mg mL$^{-1}$) under efficient stirring and deaerating. The hydrogel formed within different time.

### 2.5. Thermo-responsive behavior

The thermosensitive gel–sol transition of the hybrid solutions was determined by a vial inverted method. The aqueous solutions of each sample were placed in glass vial and then the vial was treated in a water-bath heater at specified temperature for 2 min. The thermosensitive gel–sol transition temperatures were detected by no flow (gel)–flow (sol) criterion. If no flow was observed for at least 1 min when a vial was inverted, the hydrogel was regarded as a gel state.

### 2.6. Temperature-mediated *in vitro* release kinetics studies

The CMC–BA/HCPT hydrogel was suspended in dialysis bag, and placed into PBS buffer (200 mL, pH 7.4), then incubated with shaking bath at 100 rpm at 25 °C or 37 °C, respectively. The BA and HCPT concentration was tested by obtaining periodic samples and determined by HPLC method using a reverse phase column (C18) (HCPT: 254 nm, 30 : 70 mixture (v/v) of acetonitrile–water with flow rate at 1.0 mL min$^{-1}$; BA: 210 nm, 85 : 15 mixture (v/v) of acetonitrile–water with flow rate at 1.0 mL min$^{-1}$). The amount of release was then calculated. Each sample was measured by three independent runs and calculated mean value. Drug loading content (DLC) can be calculated using the following equation: DLC (%) = (weight of loaded BA or HCPT/weight of hydrogel) × 100%.

### 2.7. Hemolysis assay

The hemolytic activity of polymer solutions was described as follows.[20] Ten milliliters of fresh blood samples were collected from mice, and then added with EDTA-$Na_2$ immediately to prevent coagulation. The red blood cells (RBCs) were collected by centrifugation at 1500 rpm for 10 min at 4 °C. After washing in ice-cold DPBS until the supernatant was clear, erythrocytes were diluted to 5 × 10$^8$ cells per mL in ice-cold DPBS. 1 mL (1 mg mL$^{-1}$ and 0.1 mg mL$^{-1}$) polymer sol sample or $PEI_{25\ K}$ solution was mixed with 1 mL erythrocyte suspension. 1% Triton X-100 in DPBS and DPBS were used as positive control (100% lysis) and negative control (0% lysis), respectively. Samples were incubated under constant shaking for 1 h at 37 °C. After centrifugation at 1500 rpm for 10 min at 4 °C, supernatant was analyzed for hemoglobin release at 541 nm using an infinite M200 microplate spectrophotometer (Tecan, Switzerland). Hemoglobin release was calculated as (absorbance of polymer samples − absorbance of negative control)/

 

(absorbance of positive control − absorbance of negative control) × 100%. Hemolysis was determined from three independent experiments.

### 2.8. *In vitro* cytotoxicity

The cell viabilities of different samples were evaluated by CCK-8 assay.[21,22] Briefly, LLC cells were seeded in 180 μL DMEM ($3 \times 10^3$ cells per well). Incubated after 24 h, the DMEM was completely removed and 200 μL of drug solutions were added to each well. Then, the cells were incubated with different drugs or materials constant temperature oven for 72 h. 20 μL of CCK-8 solution was added and continued to incubate for 1 h. Cell survival rate can be determine by calculating the absence values of the samples at 450 nm. 50% inhibitive concentration ($IC_{50}$) was computed using the Boltzmann sigmoidal function from Origin® 8.6. Data were repeated for independent tests.

### 2.9. *In vivo* antitumor activity

$3 \times 10^6$ LLC cells in 0.2 mL PBS were injected into the right axillary flank region of the mice to develop tumor xenografts. After tumor volume (TV) reaching 100 to 150 $mm^3$, treatments were initiated and this day was determined to be the day 0. From this day, thirty-six laboratory mice bearing LLC tumors were divided into 6 groups randomly, which respectively includes (a) normal saline, (b) 10 mg $kg^{-1}$ of free BA, (c) 10 mg $kg^{-1}$ of free HCPT, (d) CMC–BA/HCPT NPs (10 mg HCPT-equivalent per kg), (d) CMC–BA/HCPT hydrogel (10 mg HCPT-equivalent per kg), and (e) α-CD (100 mg $kg^{-1}$). The TV was measured every other day for 6 weeks or the implanted TV reached to 5000 $mm^3$. Using vernier calipers, measured and calculated TV, relative tumor volume (RTV), and the percentage of tumor growth inhibition (% TGI) by the formula of $TV = [\text{length} \times (\text{width})^2]/2$, $RTV = TV_t/TV_0$, $TGI = [(C - T)/C] \times 100\%$, where $TV_t$ and $TV_0$ is the TV at specified time and prior to initial treatment, respectively. $C$ and $T$ is the mean TV of the control and treatment group, respectively, at a given time point.[23,24]

### 2.10. Statistical analysis

All experiments in this study were performed at least three times, and the data were expressed as the means standard deviation (SD). Statistical analyses were performed by analysis of variance (ANOVA). In all analyses, $p < 0.05$ was taken to indicate statistical significance.

## 3. Results and discussion

### 3.1. Characterization of the CMC–BA/HCPT NPs

As previously reported,[19] the synthesis of CMC–BA prodrug is a reproducible procedure, with the optimal composition containing 29.46 ± 2.35 wt% BA (Fig. 1). The synthetic routes and chemical composition ($^1$H-NMR) of CMC–BA prodrug were shown in Fig. S1 and S2.† CMC–BA/HCPT NPs prepared from this CMC–BA prodrug were 168.5 ± 8.1 nm containing 22.95 ± 2.77 wt% BA and 22.10 ± 2.16 wt% HCPT. Fig. 2a showed the TEM images of nanoparticles.

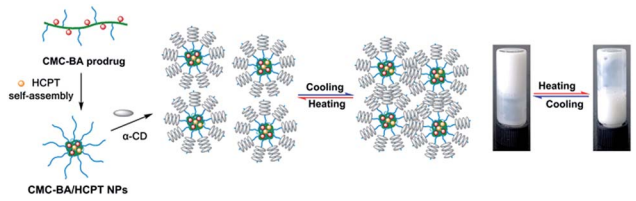


Fig. 1 Schematic of the thermosensitive hydrogel made of CMC–BA/HCPT NPs and α-CD.

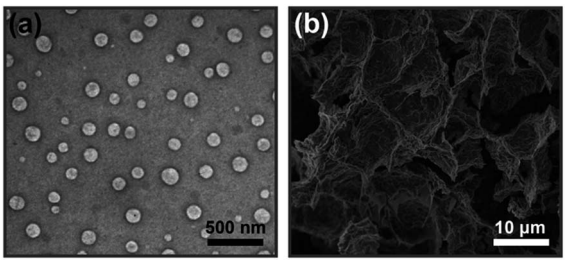


Fig. 2 TEM images of CMC–BA/HCPT NPs (a) and SEM images of the CMC–BA/HCPT hydrogel being freeze-dried (b).

### 3.2. Effect of system concentration on the gel–sol transition temperature

The temperature-responsive hydrogel was fabricated by mixing CMC–BA/HCPT NPs solutions and α-CD molecules directly, as shown in Fig. 1. The PEG were hydrophilic and mainly offered random coil structure in CMC–BA/HCPT NPs solutions. After adding α-CD molecules, the hydrogels formed by the host–guest inclusion complexation between α-CD and the PEG chains outside the nanoparticles.[25] Fig. 2b shows the SEM images of the dried CMC–BA/HCPT hydrogel. A typical porous structure was exhibited obviously from the obtained hydrogel, which is indispensable in drug delivery application allowing for drugs diffusion.[26,27]

We investigated the influence of the system concentration (α-CD and nanoparticles) on their thermo-responsive sol–gel transition behaviour. Fig. 3a and b showed the phase diagrams of CMC–BA/HCPT hydrogel formed between α-CD and CMC–BA/HCPT NPs with various concentrations. The gel–sol transition temperature ($T_{gel-sol}$) for different gels increased with the increase of the nanoparticles and α-CD concentration. Many studies have demonstrated that the process of forming PPR was summarized in the following five steps: (i) PEG chains and α-CD dispersion, (ii) PEG ends initial threading into α-CD cavities, (iii) α-CD sliding over the PEG chain, (iv) α-CD dethreading from the PEG chain, and (v) the final PPR precipitation.[28] The process of forming PPR is a dynamic equilibrium, from which we can see that the significance of the concentration of α-CD. Certain concentration of α-CD in system could slow the step (iv) to form the PPR. As the concentration of α-CD was increased, the achievement of the step (iv) was harder therefore prolonged the gelation time. On the basis of the above results, the $T_{gel-sol}$ of GEL-7 showed closer to the body temperature (Table 1). Therefore, the GEL-7 with a 1.98 wt% BA and 1.90 wt% HCPT loading efficiency was chosen for the following properties characterization and anti-tumor activity assay.

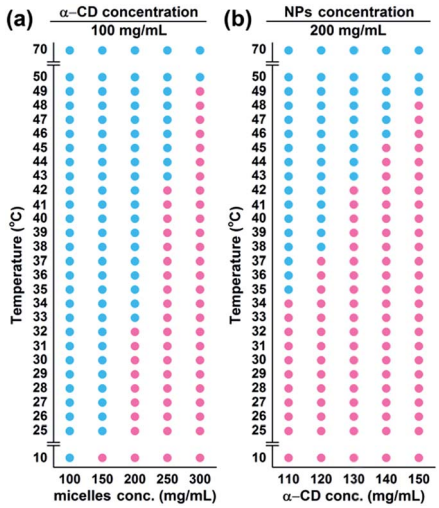


Fig. 3 Thermosensitive sol–gel transition behavior. ●: sol, ●: gel.

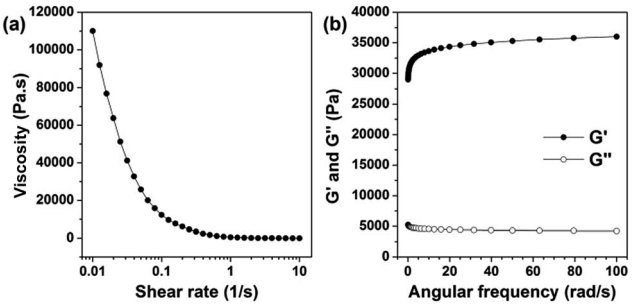


Fig. 4 (a) Dynamic and (b) steady rheological behaviors of the GEL-7.

### 3.3. Viscoelastic behaviour of CMC–BA/HCPT hydrogel

Fig. 4a and b showed the viscoelastic behaviour of the hydrogel which was measured by dynamic mechanical measurements. As a kind of elastomeric hydrogel, the storage modulus ($G'$) and the loss modulus ($G''$) of gel-2 increased and decreased slowly, respectively, in the range of whole frequency. And as expected, the $G'$ is about one order of magnitude higher than the $G''$ (Fig. 4a). Moreover, when the shear rate increased, the viscosity of the hydrogel dramatically dropped (Fig. 4b). The viscosity showed a remarkable shear-thinning effect. The viscosity showed a remarkable shear-thinning effect. The uniformly distributed hydrophobic nanoparticles core and the hydrophobic–hydrophobic interactions between the HCPT and BA molecules inner shell of the nanoparticles can improve the strength of the hydrogels to a certain extent.[29] Thus, for these viscoelasticity, the CMC–BA/HCPT hydrogel can be an efficient injectable material for drug delivery.

### 3.4. *In vitro* release of BA and HCPT

*In vitro* release kinetic of BA and HCPT from CMC–BA/HCPT hydrogel which affected by temperature was quantified by HPLC analysis (Fig. 5a and b). When the incubation temperature increases from 25 °C to 37 °C, hydrogel release rates showed obvious accelerating phenomenon. This accelerated release was attributed to the sol state of the temperature responsive hydrogel. These release properties can be a benefit to the enhanced cytotoxicity *in vivo* and stable *in vitro*. However, the hydrogels rapidly hydrolyzed and released the drugs in the presence of esterase (abundant in cytoplasm).[30] Therefore, CMC–BA/HCPT hydrogel in sol state were prodrugs for intracellular release of BA.

An empirical power equation has been proposed to explain the behaviors of drug release.[31,32] The equation is written as: $\log(M_t/M_\infty) = n \log t + \log k$, where $M_t$ and $M_\infty$ are the cumulative amount of drug released at time $t$ and infinite time, respectively, $k$ is a constant incorporating structural and geometric characteristics of the device, and $n$ is the release exponent, indicative of the mechanism of drug release.

When $n$ has value 0.45 or 0.89, the drug release behavior was called Fickian diffusion or case-II transport, and indicated diffusion-controlled release or swelling-controlled release, respectively.[33] When $n$ is between 0.45 and 0.89, the drug release behavior was called anomalous transport which can be viewed as the superposition of both phenomena.

$\log(M_t/M_\infty)$ *versus* $\log t$ of the experimental data has been plotted according to the equation. Fig. 5c and d shows a typical plot of $\log(M_t/M_\infty)$ against $\log t$ in hydrogel at 25 °C and 37 °C. Good linear relation indicated that the Peppas's equation is suitable to this hydrogel system. By these plots, Table 2 shows the values of $n$ and $\log k$ for the CMC–BA/HCPT hydrogel. The $n$ values for BA and HCPT are all much smaller than 0.89 and

Table 1 The gel–sol transition temperature and drug loading efficiency of the hydrogel

| Gels | Nanoparticles (mg mL$^{-1}$) | α-CD (mg mL$^{-1}$) | $T_{gel-sol}$ (°C) | $DLE_{BA}$ (wt%) | $DLE_{HCPT}$ (wt%) |
|---|---|---|---|---|---|
| GEL-1 | 100 | 100 | — | 1.04 | 1.00 |
| GEL-2 | 150 | 100 | 25 | 1.53 | 1.47 |
| GEL-3 | 200 | 100 | 33 | 2.00 | 1.92 |
| GEL-4 | 250 | 100 | 43 | 2.44 | 2.35 |
| GEL-5 | 300 | 100 | 50 | 2.87 | 2.76 |
| GEL-6 | 200 | 110 | 35 | 1.99 | 1.91 |
| GEL-7 | 200 | 120 | 38 | 1.98 | 1.90 |
| GEL-8 | 200 | 130 | 43 | 1.97 | 1.90 |
| GEL-9 | 200 | 140 | 46 | 1.96 | 1.89 |
| GEL-10 | 200 | 150 | 49 | 1.95 | 1.88 |

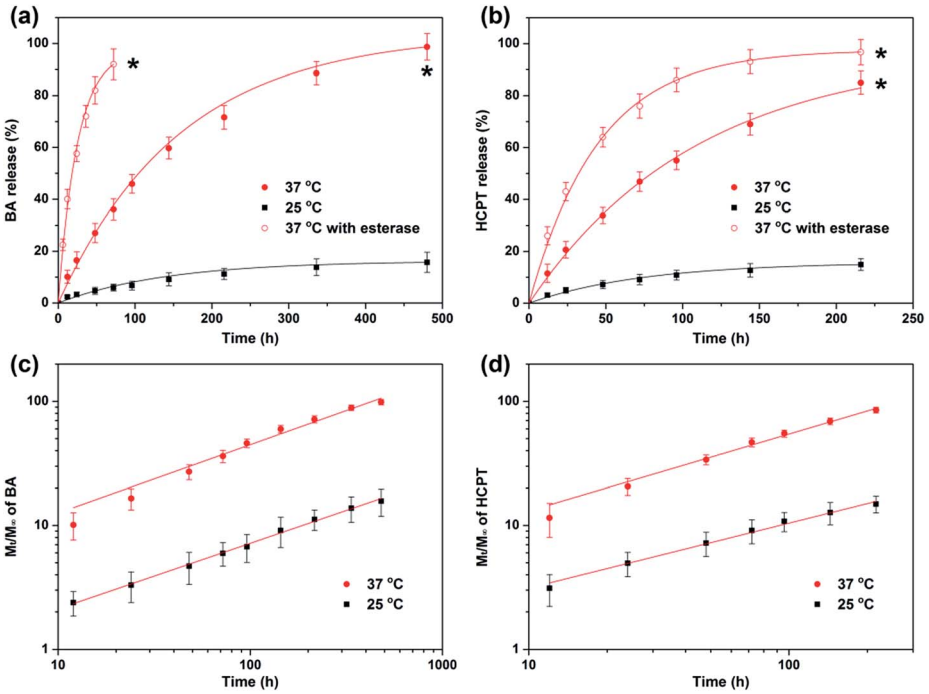


Fig. 5 BA (a) and HCPT (b) release from GEL-7. Plots of $\log(M_t/M_\infty)$ against $\log t$ for BA (c) and HCPT (d) release from the GEL-7 at 25 °C and 37 °C.

Table 2 Caption release exponent ($n$), rate constant ($\log k$), and correlation coefficient ($R^2$) for hydrogel[9]; $T = 25$ °C and 37 °C

| Drug | $T$ (°C) | $\log k$ | $n$ | $R^2$ |
|---|---|---|---|---|
| BA | 25 | −0.20 | 0.53 | 0.99 |
| | 37 | 0.55 | 0.55 | 0.99 |
| HCPT | 25 | −0.03 | 0.52 | 0.99 |
| | 37 | 0.62 | 0.50 | 0.99 |

greater than 0.45, indicating that the release is anomalous transport. The release mechanism suggests that the nanoparticles have a influence on the drugs in their release process.[32] The values of $\log k$ for BA and HCPT as significantly increased as the temperature increased which indicated thermosensitivity of the release rate.

### 3.5. Hemolysis study

Harmful interaction of nanoparticles and hydrogel with RBCs must be avoided when these drug formulations enter the bloodstream.[34] Hemolysis was detected and the results were shown in Fig. 6. As the positive control, Triton X-100 induced full hemoglobin release. Drug-loading nanoparticles and hydrogel (gel-2) at different concentrations showed a extremely low hemoglobin release (<5%), which comparable to blank values and significantly lower than the same concentrations of $PEI_{25\ K}$. Despite HCPT and BA has certain toxicity to the RBCs in earlier studies,[35,36] the hydrogel has been released small amounts of free drugs during the short incubation period, suggesting the reliable security of the hydrogel.

### 3.6. *In vitro* cytotoxicity

Cytotoxicity of the GEL-7 on LLC cells was determined by the CCK-8 assay. Previous studies have shown that cytotoxicity is related with duration of drug treatment. In order to compare the effect of drug formulations, the $IC_{50}$ after 72 h were obtained from survival curves as shown in Fig. 7. The results showed that the $IC_{50}$ of the sample is in the order free BA > free HCPT > CMC–BA/HCPT NPs > CMC–BA/HCPT hydrogel.

Compared to the free BA treatment, the CMC–BA/HCPT NPs and hydrogel (GEL-7) treatment was 29.7 and 40.5 times more toxic than LLC, respectively. Compared to the free HCPT, the CMC–BA/HCPT NPs and hydrogel (GEL-7) treatment was 1.7 and 2.4 times more toxic than LLC, respectively (Table 3). The increased toxicities of CMC–BA/HCPT NPs and GEL-7 were approximately related to the slow release of the drugs. Beyond

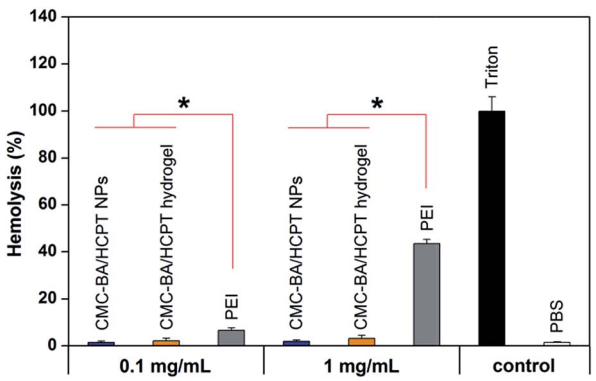


Fig. 6 Hemolysis assay of nanoparticles and hydrogel (GEL-7).

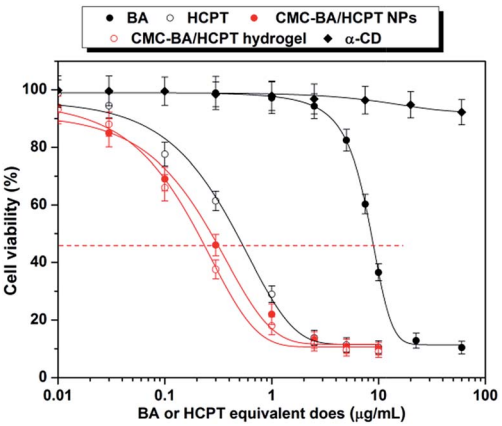


Fig. 7 Cell viability and $IC_{50}$ of LLC cells treated with different concentrations of the samples.

Table 3 *In vitro* cytotoxicity analysis

| Compound | $IC_{50}$, μg $mL^{-1}$ |
|---|---|
| α-CD | — |
| BA | 8.92 (0.50287) |
| HCPT | 0.52 (0.02936) |
| CMC–BA/HCPT NPs | 0.30 (0.02015) |
| CMC–BA/HCPT hydrogel (GEL-7) | 0.22 (0.01357) |

the advantages of slow release, the combined treatment with BA and HCPT can improve *in vitro* therapeutic effectiveness significantly *versus* a single drug. Both HCPT and BA are potent Topoisomerase (Top) inhibitors, but HCPT just interferes with the action of Top I. Certain clinical limitations such as resistance of cancer cells impair its clinical application.[15] It has been proven that the increase of Top II activity occurs in cancer cells resistant to HCPT.[16] BA has been reported to be a catalytic inhibitor of TOP I and II activity. Top II inhibitor shows a collateral cytotoxicity on the HCPT adapted cancer cells. Therefore, the concomitant use of both Top I and Top II inhibitors might elicit synergistic effects and prevent the emergence of drug resistance. We evaluate the synergistic effects between BA and HCPT in GEL-7 by applying the combination index (CI) used in the combination treatment. CI = $BA_{combined}/BA_{single}$ + $HCPT_{combined}/HCPT_{single}$, whereby $BA_{combined}$ and $HCPT_{combined}$ represent the $IC_{50}$ of drugs, and $BA_{single}$ and $HCPT_{single}$ represents single drug $IC_{50}$. The CI value lesser or larger than 1 indicated a synergistic or an antagonistic effect, respectively. GEL-7 $IC_{50}$ of LLC cells was 0.22 μg $mL^{-1}$, the calculated CI value of BA and HCPT in GEL-7 were 0.45, which suggested that GEL-7 achieve the cooperative action of BA and HCPT.[37]

### 3.7. *In vivo* antitumor activity

Although various kinds of drug delivery systems emerged endlessly, localized therapy is a very effective cure for cancers.[38–40] Accordingly, we investigated GEL-7 for localized BA and HCPT delivery by an effective and simple peritumoral injection strategy. Tumor-bearing mice treated with GEL-7 achieved higher survival rate than the other groups (Fig. 8b). On the other hand, the treatment of saline (negative control) or α-CD showed hardly therapeutic effect. Injection of free BA and HCPT could have a certain degree of efficacy, but only days later the tumor was growing uncontrollably. Oppositely, the injection of the nanoparticles and GEL-7, particularly GEL-7, inhibited the growth of tumor obviously during this experimental period

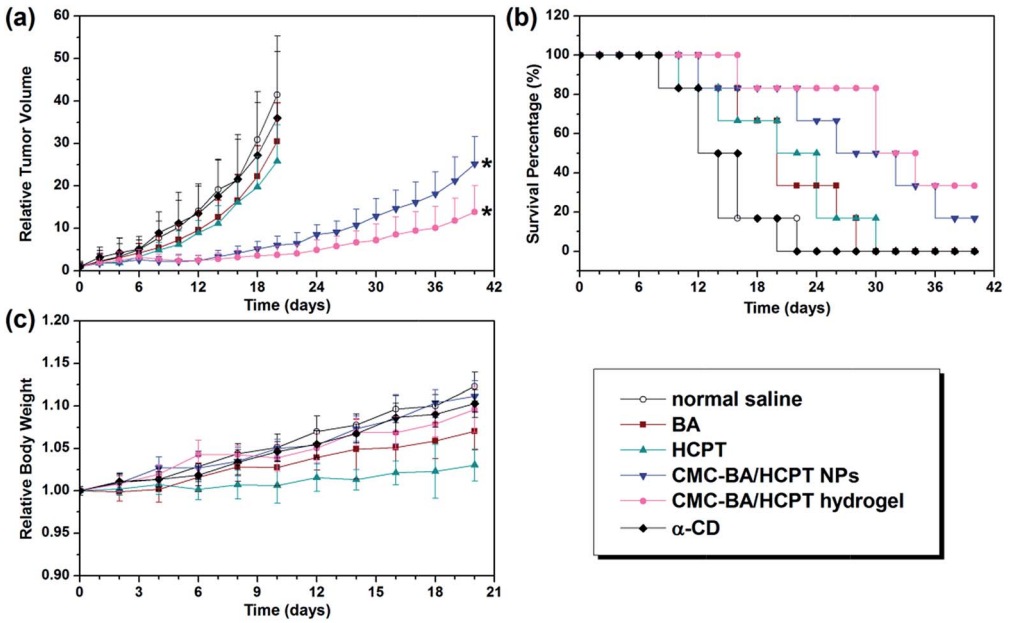


Fig. 8 *In vivo* antitumor activity of the samples in the subcutaneous mouse model of LLC. (a) Tumor volumes of mice during treatment with different groups. (b) Survival of mice in different treatment. (c) The animal weights were recorded once per week and expressed over the 20 day observation.

 

Table 4 The antitumor efficacy of different groups

| Compound | Mean TV ± SD[a] ($mm^3$) | RTV[a] | TGI[a] (%) | Cures[b] (%) |
|---|---|---|---|---|
| Normal saline | 5436 ± 1808 | 41.5 ± 13.8 | 0 | 0 |
| α-CD | 4968 ± 2153 | 36.0 ± 15.6 | 8.6 | 0 |
| BA | 3690 ± 1101 | 30.5 ± 9.1 | 32.1 | 16.7 |
| HCPT | 3328 ± 1109 | 25.8 ± 8.6 | 38.8 | 16.7 |
| CMC–BA/HCPT NPs | 781 ± 282 | 6.1 ± 2.2 | 85.6 | 50.0 |
| GEL-7 | 502 ± 238 | 3.8 ± 1.8 | 90.8 | 83.3 |

[a] 20 days of mean TV, RTV, and TGI data. [b] 28 days of cures data.

(Table 4, Fig. 8a). And best of all, no signs of systemic toxicity were found in the monitored general behavior, appetite and body weight (Fig. 8c). The better therapeutic effects of the GEL-7 may be anticipated on the basis of the following reasons: (1) GEL-7 have excellent sustained release of drugs, (2) nanoparticles in GEL-7 has the appropriate size (~150 nm), which can lead more nanoparticles to be accumulated at the tumor site *via* the EPR effect,[41] and (3) drug-loaded hydrogel and nanoparticles can improve the drugs poor solubility to some extent.[42] All these results suggest that the BA and HCPT-loaded gel-2 could be a safe and effect candidate formulation for delivery anticancer drugs and suppression of tumor growth.

## 4. Conclusion

An injectable and thermosensitive drug delivery system from CMC–BA/HCPT NPs/α-CD hydrogel has been prepared by a combination of the host–guest inclusion complexation between α-CD and the PEG chains outside the nanoparticles. The structure and thermosensitivity of PPR could be controlled simply by varying the concentration of the nanoparticles and α-CD. GEL-7, the $T_{gel-sol}$ closer to the body temperature, was chosen for the following studies. The obtained release profiles of hydrogel are well fitted by the classical empirical power law. In addition, this injectable hydrogel showed appealing properties as an anticancer drug delivery system consist of simple preparation, good thermosensitive, high loading capacity, favorable stability, long release profile, good antitumor activity *in vitro* and *in vivo*, and low systemic toxicity. This work may promote the nano-materials and injectable hydrogel for drug delivery.

## Acknowledgements

This work was financially supported by the State Key Laboratory of Tree Genetics and Breeding, State Key Laboratory of Pulp and Paper Engineering (201611), Jiangsu Province Biomass Energy and Materials Laboratory in Institute of Chemical Industry of Forest Products, CAF (JSBEM201601).

## Notes and references

1 H. Kuang, H. He, Z. Zhang, Y. Qi, Z. Xie, X. Jing and Y. Huang, *J. Mater. Chem. B*, 2014, **2**, 659–667.
2 E. A. Appel, J. del Barrio, X. J. Loh and O. A. Scherman, *Chem. Soc. Rev.*, 2012, **41**, 6195–6214.
3 K. Miyamae, M. Nakahata, Y. Takashima and A. Harada, *Angew. Chem., Int. Ed.*, 2015, **54**, 8984–8987.
4 Y. Guan, J. Bian, F. Peng, X.-M. Zhang and R.-C. Sun, *Carbohydr. Polym.*, 2014, **101**, 272–280.
5 S. Merino, C. Martin, K. Kostarelos, M. Prato and E. Vazquez, *ACS Nano*, 2015, **9**, 4686–4697.
6 Y. Miura, T. Takenaka, K. Toh, S. Wu, H. Nishihara, M. R. Kano, Y. Ino, T. Nomoto, Y. Matsumoto, H. Koyama, H. Cabral, N. Nishiyama and K. Kataoka, *ACS Nano*, 2013, **7**, 8583–8592.
7 H. Cabral and K. Kataoka, *J. Controlled Release*, 2014, **190**, 465–476.
8 M. Talelli, M. Barz, C. J. F. Rijcken, F. Kiessling, W. E. Hennink and T. Lammers, *Nano Today*, 2015, **10**, 93–117.
9 N. Kamaly, Z. Xiao, P. M. Valencia, A. F. Radovic-Moreno and O. C. Farokhzad, *Chem. Soc. Rev.*, 2012, **41**, 2971–3010.
10 H. Wei, R.-X. Zhuo and X.-Z. Zhang, *Prog. Polym. Sci.*, 2013, **38**, 503–535.
11 R. Duncan, *Nat. Rev. Drug Discovery*, 2003, **2**, 347–360.
12 A. K. Gaharwar, N. A. Peppas and A. Khademhosseini, *Biotechnol. Bioeng.*, 2014, **111**, 441–453.
13 N. Annabi, A. Tamayol, J. A. Uquillas, M. Akbari, L. E. Bertassoni, C. Cha, G. Camci-Unal, M. R. Dokmeci, N. A. Peppas and A. Khademhosseini, *Adv. Mater.*, 2014, **26**, 85–124.
14 P. Thoniyot, M. J. Tan, A. A. Karim, D. J. Young and X. J. Loh, *Adv. Sci.*, 2015, **2**, 1400010.
15 J. Li and X. J. Loh, *Adv. Drug Delivery Rev.*, 2008, **60**, 1000–1017.
16 A. Harada, A. Hashidzume, H. Yamaguchi and Y. Takashima, *Chem. Rev.*, 2009, **109**, 5974–6023.
17 J. Li, X. Ni and K. W. Leong, *J. Biomed. Mater. Res., Part A*, 2003, **65**, 196–202.
18 M. Ceccato, P. Lo Nostro and P. Baglioni, *Langmuir*, 1997, **13**, 2436–2439.
19 L. Dai, K.-F. Liu, C.-L. Si, J. He, J.-D. Lei and L.-Q. Guo, *J. Mater. Chem. B*, 2015, **3**, 6605–6617.
20 R. Reul, J. Nguyen and T. Kissel, *Biomaterials*, 2009, **30**, 5815–5824.
21 D. Ni, H. Ding, S. Liu, H. Yue, Y. Bao, Z. Wang, Z. Su, W. Wei and G. Ma, *Small*, 2015, **11**, 2518–2526.
22 L. Dai, K. Liu, C. Si, L. Wang, J. Liu, J. He and J. Lei, *J. Mater. Chem. B*, 2016, **4**, 529–538.
23 K. Dong, Z. Liu, Z. Li, J. Ren and X. Qu, *Adv. Mater.*, 2013, **25**, 4452–4458.
24 A. J. Souers, J. D. Leverson, E. R. Boghaert, S. L. Ackler, N. D. Catron, J. Chen, B. D. Dayton, H. Ding, S. H. Enschede, W. J. Fairbrother, D. C. S. Huang, S. G. Hymowitz, S. Jin, S. L. Khaw, P. J. Kovar, L. T. Lam, J. Lee, H. L. Maecker, K. C. Marsh, K. D. Mason, M. J. Mitten, P. M. Nimmer, A. Oleksijew, C. H. Park, C.-M. Park, D. C. Phillips, A. W. Roberts, D. Sampath, J. F. Seymour, M. L. Smith, G. M. Sullivan, S. K. Tahir, C. Tse, M. D. Wendt, Y. Xiao, J. C. Xue, H. Zhang,

R. A. Humerickhouse, S. H. Rosenberg and S. W. Elmore, *Nat. Med.*, 2013, **19**, 202–208.
25 X. Ma and Y. Zhao, *Chem. Rev.*, 2015, **115**, 7794–7839.
26 J. He, M. Zhang and P. Ni, *Soft Matter*, 2012, **8**, 6033–6038.
27 X. Huang and C. S. Brazel, *J. Controlled Release*, 2001, **73**, 121–136.
28 M. Arunachalam and H. W. Gibson, *Prog. Polym. Sci.*, 2014, **39**, 1043–1073.
29 H. Zou, W. Guo and W. Yuan, *J. Mater. Chem. B*, 2013, **1**, 6235–6244.
30 Y. Shen, E. Jin, B. Zhang, C. J. Murphy, M. Sui, J. Zhao, J. Wang, J. Tang, M. Fan, E. Van Kirk and W. J. Murdoch, *J. Am. Chem. Soc.*, 2010, **132**, 4259–4265.
31 P. L. Ritger and N. A. Peppas, *J. Controlled Release*, 1987, **5**, 23–36.
32 J. Siepmann and N. A. Peppas, *Adv. Drug Delivery Rev.*, 2001, **48**, 139–157.
33 P. Colombo, R. Bettini, P. L. Catellani, P. Santi and N. A. Peppas, *Eur. J. Pharm. Sci.*, 1999, **9**, 33–40.
34 J. G. Schellinger, J. A. Pahang, R. N. Johnson, D. S. H. Chu, D. L. Sellers, D. O. Maris, A. J. Convertine, P. S. Stayton, P. J. Horner and S. H. Pun, *Biomaterials*, 2013, **34**, 2318–2326.
35 M. Gao, P. M. Lau and S. K. Kong, *Arch. Toxicol.*, 2014, **88**, 755–768.
36 Z. Su, J. Niu, Y. Xiao, Q. Ping, M. Sun, A. Huang, W. You, X. Sang and D. Yuan, *Mol. Pharmaceutics*, 2011, **8**, 1641–1651.
37 T.-C. Chou, *Cancer Res.*, 2010, **70**, 440–446.
38 N. Bhattarai, J. Gunn and M. Zhang, *Adv. Drug Delivery Rev.*, 2010, **62**, 83–99.
39 O. P. Varghese, W. Sun, J. Hilborn and D. A. Ossipov, *J. Am. Chem. Soc.*, 2009, **131**, 8781–8783.
40 Y. Yang, J. Wang, X. Zhang, W. Lu and Q. Zhang, *J. Controlled Release*, 2009, **135**, 175–182.
41 H. Maeda, *Adv. Drug Delivery Rev.*, 2015, **91**, 3–6.
42 O. P. Medina, N. Pillarsetty, A. Glekas, B. Punzalan, V. Longo, M. Gönen, P. Zanzonico, P. Smith-Jones and S. M. Larson, *J. Controlled Release*, 2011, **149**, 292–298.